NACA RM E54C23

NACA

RESEARCH MEMORANDUM

PERFORMANCE OF WEDGE-TYPE BOUNDARY LAYER DIVERTERS FOR SIDE INLETS AT SUPERSONIC SPEEDS

By Robert C. Campbell and Emil J. Kremzier

Lewis Flight Propulsion Laboratory
Cleveland, Ohio

NATIONAL ADVISORY COMMITTEE
FOR AERONAUTICS
WASHINGTON

May 13, 1954
Declassified July 22, 1959

NATIONAL ADVISORY COMMITTEE FOR AERONAUTICS

RESEARCH MEMORANDUM

PERFORMANCE OF WEDGE-TYPE BOUNDARY-LAYER DIVERTERS FOR SIDE INLETS AT SUPERSONIC SPEEDS

By Robert C. Campbell and Emil J. Kremzier

SUMMARY

An experimental investigation to determine the effect of several wedge-type boundary-layer diverters on drag and inlet pressure recovery has been conducted in the Lewis 8- by 6-foot supersonic wind tunnel at free-stream Mach numbers of 1.5, 1.8, and 2.0. The model investigated consisted of two rectangular ramp-type inlets mounted on the NACA RM-10 body of revolution.

Results indicated that for wedges of 60° and 100° included angle, inlet-body drag was 9 to 15 percent higher than for wedges of 16° included angle. Since increases in diverter wedge angle increased the model drag with some decrease in inlet pressure recovery for the higher angles in their forward position, it appears aerodynamically desirable to keep the diverter included angle at or near 16°. Ducted wedges showed increases in drag over most of the comparable closed-wedge configurations and an increase in pressure recovery over comparable closed-wedge diverters at the inlet ramp leading edge.

INTRODUCTION

Efficient performance of a side inlet obtained through removal of the fuselage boundary layer ahead of the inlet is usually accompanied by increases in configuration drag which at least partially offset the benefits of improved inlet performance. Recent studies that have been undertaken to evaluate the relative merits of various boundary-layer diverter systems have presented either the effects on inlet performance (ref. 1) or the variation of diverter pressure drag (ref. 2).

In order to determine and relate the effects on both total drag and inlet performance of the angle and longitudinal position of closed- and ducted-wedge-type boundary-layer diverters, an investigation was conducted in the NACA 8- by 6-foot supersonic wind tunnel. A series of diverter

configurations was tested at free-stream Mach numbers of 1.5, 1.8, and 2.0 in conjunction with two horizontally opposed ramp-type side inlets mounted on the NACA RM-10 body of revolution.

SYMBOLS

The following symbols are used in this report:

A_f	maximum frontal area of model, 0.2765 sq ft
A_i	inlet capture area, 0.0233 sq ft
C_D	external drag coefficient based on maximum frontal area, drag/$q_0 A_f$
C_{D_p}	wedge pressure drag coefficient based on frontal area of diverter
m_2/m_0	inlet-diffuser mass-flow ratio, $\frac{\text{inlet-diffuser mass flow}}{\rho_0 V_0 A_i}$
P	total pressure, lb/sq ft
q	dynamic pressure, lb/sq ft
r	body radius, in.
s	distance from leading edge of ramp to vertex of diverter, in.
V	velocity, ft/sec
x	body station
δ	boundary-layer thickness, in.
θ	wedge diverter included angle, deg
ρ	mass density of air

Subscripts:

0	free stream
2	diffuser-discharge survey station, model station 66.5

APPARATUS AND PROCEDURE

A schematic diagram of the model is presented in figure 1. Two rectangular-type inlets were mounted horizontally opposed on the RM-10 body of revolution with their cowl lips at fuselage station 45.

Details of the boundary-layer diverter configurations tested are shown, and wedge angles and longitudinal positions are tabulated in figure 2. Vertices of the closed wedges were located longitudinally at the inlet ramp leading edge, 0.4 inch aft (1 boundary-layer thickness) and 0.8 inch aft of the ramp leading edge. Ducted-wedge vertices were located at zero and 0.4 inch aft of the ramp leading edge. The ducted wedges at their leading edges had duct widths equal to one-third the inlet width. Captured boundary-layer mass flow was then ducted to the side approximately 6 inches downstream (fig. 2(b)). The boundary-layer bleed height of 0.4 inch used throughout the test was approximately equal to the boundary-layer thickness at zero angle of attack, while diverter frontal areas were about 0.0082 square foot.

Details of the inlet and variations in the diffuser cross section are shown in figure 3. The 14° compression surface was curved to conform to the local body radius, and the internal cowl-lip angle was 12°. The inlet was designed so that the oblique shock generated by the leading edge of the ramp would fall slightly ahead of the cowl lip at a free-stream Mach number of 2.0. Capture area of each inlet was 0.0233 square foot and the total capture area of both inlets comprised about 23.7 percent of the basic fuselage frontal area. Internal fillets were used to eliminate sharp corners in the subsonic diffuser. Variation of the diffuser flow area is shown in figure 4.

The model was sting supported and connected to the sting by a three-component internal strain-gage balance that measured normal and axial forces and pitching moment. The balance moment center was located at station 45 on the body center line. Inlet mass flow was varied by means of remotely controlled movable tail-pipe plugs attached to the sting.

Pressure instrumentation consisted of 19 total-pressure tubes and six wall static-pressure orifices in each diffuser at body station 66.5, base-pressure orifices, chamber-pressure orifices located in the model balance cavity, and static-pressure orifices on the surface of the boundary-layer diverter wedges of one inlet.

Inlet mass-flow ratio was determined from the diffuser-discharge Mach number and average total pressure. The diffuser-discharge Mach number was obtained from the known area ratio between the diffuser-discharge station and the exit plug, which was assumed to be choked. Average total pressure was calculated by area weighting the total-pressure measurements.

The forces resulting from the change in inlet-air momentum from free stream to diffuser exit and base forces resulting from the difference in base pressure from free-stream static pressure have been excluded from the model force data. In order to reduce the internal duct forces and thereby improve the calculations of external drag, fixed nozzle blocks were inserted in the diffuser exits for most of the test. Diffuser-discharge Mach number with nozzle inserts was maintained at about 0.21, thus assuring supercritical inlet operation at free-stream Mach numbers of 1.8 and 2.0.

With nozzle inserts, the angle of attack was varied from zero to 10° at free-stream Mach numbers of 1.5, 1.8, and 2.0. For three closed-wedge configurations and all ducted-wedge configurations, inlet mass-flow ratio was varied at zero angle of attack over the same Mach number range. Reynolds number varied from 24×10^{6} to 30×10^{6} based on model length.

RESULTS AND DISCUSSION

Variation of inlet pressure recovery and configuration drag with inlet mass-flow ratio is presented in figure 5 for the three closed-wedge configurations for which mass flow was varied. Pressure-recovery mass-flow data at a diffuser-discharge Mach number of 0.21, obtained for all wedge configurations while the diffuser-exit nozzle blocks were in place, are presented in figure 5 for two closed-wedge configurations at a free-stream Mach number of 2.0. For all other configurations and Mach numbers, nozzle-block data coincided with the data for variable mass flow. Inlet pressure-recovery and mass-flow characteristics were not appreciably affected by changes in the wedge angle from 16° to 60° for wedges located 1 boundary-layer thickness aft of the ramp leading edge (s/δ of 1). Configuration drag, however, did increase. Inlet pressure recovery and configuration drag were unaffected by a change in longitudinal position of the 60° diverter from s/δ of 2 to s/δ of 1. Nozzel-block data obtained at a diffuser-discharge Mach number of 0.2, however, indicated a decrease in pressure recovery at a free-stream Mach number of 2.0 when the 60° and 100° diverters were placed at the inlet ramp leading edge (s/δ of 0). Similar adverse effects of wedge position on inlet pressure recovery at Mach numbers of 1.5 and 1.7 are reported in reference 1 for 100° diverters.

Changes in the shock pattern off the inlet ramp for changes in diverter angle can be seen in the schlieren photographs of figures 6(a) and (b). For the longitudinal positions shown, increasing the wedge angle appears to form disturbances ahead of the inlet ramp, though no changes in inlet performance were observed for these configurations.

A separated flow region with an associated oblique shock is visible on the ramp surface in the photograph of subcritical inlet flow (fig. 6(a), θ of 16°). This separated flow region was observed, for all wedge configurations investigated, at Mach numbers of 1.8 and 2.0. It is shown in reference 1 that elimination or reduction of inlet ramp separation can improve inlet performance. However, reductions in pressure recovery for the improved inlet of reference 1 were greater for similar changes in boundary-layer configurations than were those shown for the inlet reported herein.

Pressure-recovery - mass-flow characteristics for all ducted wedges were approximately the same as those for the closed wedges for values of s/δ other than zero (fig. 5). Since, however, the 60° included-angle closed-wedge diverter at s/δ of 0 showed reductions in pressure recovery previously discussed in this section, some improvement is apparent in going from this configuration to the comparable 30° half-angle ducted wedge in the same position. Figure 6(c), which shows the diverters at s/δ of 1.0, shows a lesser degree of influence on the inlet shock pattern for the ducted wedge than for its comparable closed-wedge diverter though pressure-recovery - mass-flow characteristics for these two configurations are identical.

Wedge pressure drag coefficients based on wedge frontal area are presented in figure 7 as a function of angle of attack. The values shown on the curves were substantially independent of mass-flow ratio. Variations in wedge pressure drag with angle of attack are slight compared with model total drag at similar angles of attack. However, significant pressure drag increases are noted with increases in wedge included angle.

In figure 8 is shown a more detailed effect of wedge included angle on model total drag coefficient (solid curves), together with a drag breakdown including body plus inlet drag, and body plus inlet plus wedge pressure drag (dashed curves). Model total drags in figures 8 and 9 were obtained at a diffuser-discharge Mach number of 0.21 with nozzle blocks installed. The drag of the body plus inlets was obtained by subtracting the drag increment between h/δ of 0 and h/δ of 1.0 measured for the model of reference 3 from the total drag of the 16° wedge configuration of this investigation. The dashed curves were obtained by adding the measured wedge pressure drag to the drag of the body plus inlets. The drag increment between the dashed and solid curves represents the sum of the wedge friction drag and all other pressure and friction drags resulting from the radial translation of the inlets from h/δ of 0 to h/δ of 1.0.

The pressure drag of the 16° wedge is negligible compared with the total drag of the model. Wedge friction drag plus translation drag decreases with increasing wedge angle. If the translation drag is

assumed to be small, the relative proportions of wedge pressure and friction drag are comparable with those presented in figure 8 of reference 2. Increases in wedge included angle from 16° to 60° resulted in increases in total drag of 9 to 15 percent. Only slight increases in total drag were obtained for increases in wedge angle above 60°. Since increases in diverter wedge angle increased the model drag and decreased to some extent the inlet pressure recovery at the higher wedge angles, it appears aerodynamically desirable to keep the wedge diverter angle at or near 16°.

A comparison of model drag coefficients for the closed- and ducted-wedge configurations is presented in figure 9. The higher drags for the ducted wedges are probably caused by increases in friction drag due to the greater wetted surface area. A comparison of closed- and ducted-wedge diverters of 60° included angle in the forward position, s/δ of 0, indicates a higher pressure recovery for the ducted wedge at a free-stream Mach number of 2.0 and slightly higher drag, at least for the lower Mach numbers. For comparable closed- and ducted-wedge diverter angles at s/δ of 1.0, no difference in pressure recovery was noted though drags for the ducted-wedge diverters were again slightly higher. For the inlet of reference 1, however, ducted wedges showed improvements in inlet pressure recovery over closed-wedge configurations of similar wedge angles yet no measurable differences in drag were observed.

SUMMARY OF RESULTS

An investigation was conducted to compare performances of several wedge-type boundary-layer diverter systems at Mach numbers from 1.5 to 2.0. The following results were obtained:

1. Increases in boundary-layer diverter angle from 16° to 60° and 100° resulted in increases in total model drag of 9 to 15 percent. Some decrease in inlet pressure recovery with increase in wedge angle was noted at the higher diverter angles in their forward position. It thus appears aerodynamically desirable to keep the diverter wedge angle at or near 16°, while higher-angle wedge diverters should be located with their leading edges aft of the inlet ramp leading edge to avoid adverse effects on inlet pressure recovery.

2. For the ducted wedges, slight increases in drag were apparent over most of the comparable closed-wedge diverters with slight increases in pressure recovery over comparable closed-wedge diverters located at the inlet ramp leading edge.

Lewis Flight Propulsion Laboratory
National Advisory Committee for Aeronautics
Cleveland, Ohio, March 19, 1954

REFERENCES

1. Obery, Leonard J., and Stitt, Leonard E.: Investigation at Mach Numbers 1.5 and 1.7 of Twin-Duct Side Air-Intake Systems with 9^{o} Compression Ramp Including Modifications to Boundary-Layer-Removal Wedges and Effects of a Bypass System. NACA RM E53H04, 1953.

2. Piercy, Thomas G., and Johnson, Harry W.: Experimental Investigation at Mach Numbers 1.88, 3.16, and 3.83 of the Pressure Drag of Wedge Diverters Simulating Boundary-Layer-Removal Systems for Side Inlets. NACA RM E53L14b, 1954.

3. Valerino, Alfred S., Pennington, Donald B., and Vargo, Donald J.: Effect of Circumferential Location on Angle of Attack Performance of Twin Half-Conical Scoop-Type Inlets Mounted Symmetrically on the RM-10 Body of Revolution. NACA RM E53G09, 1953.

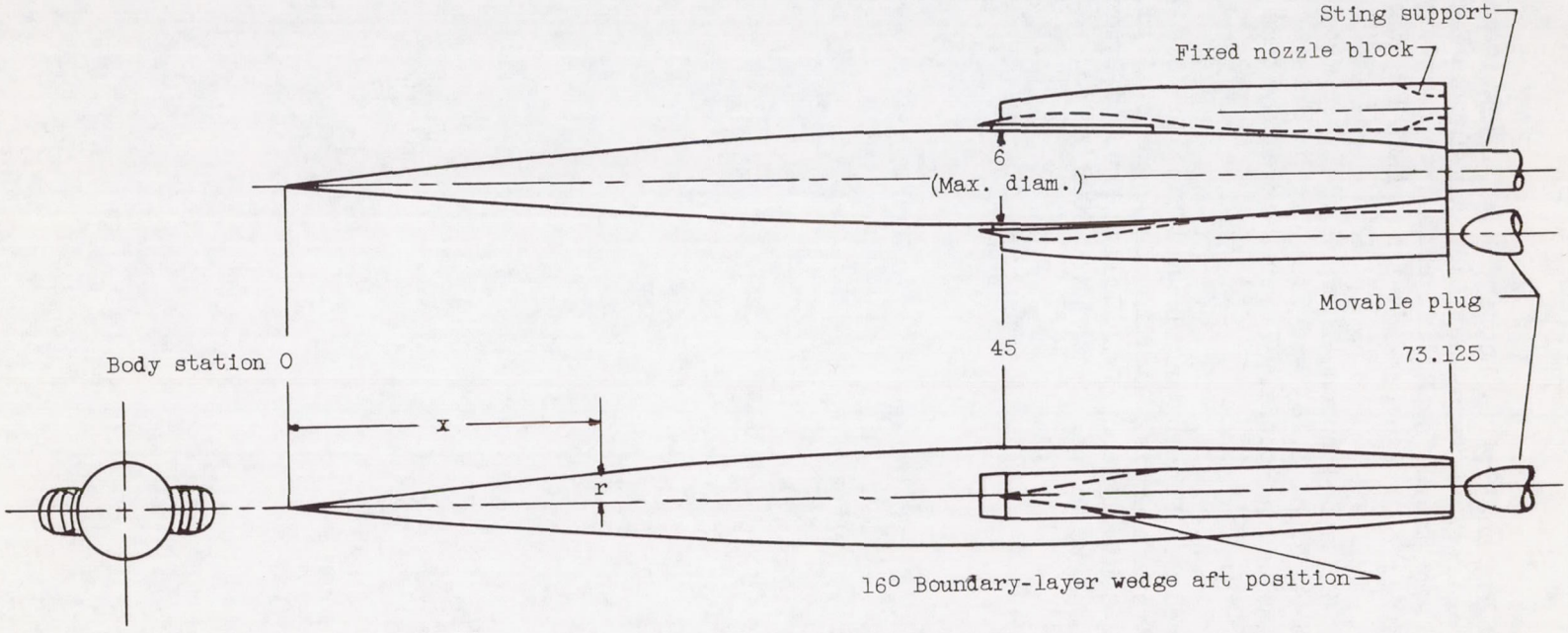

Figure 1. - Sketch of model investigated. RM-10 body defined by $r = \frac{x}{15}\left(2 - \frac{x}{45}\right)$. (Dimensions are in inches.)

Closed wedge			Ducted wedge		
Position		Included angle	Position		Half angle
s, in.	s/δ	θ, deg	s, in.	s/δ	θ/2, deg
0	0	16, 60, 100	0	0	30
.4	1	16, 60, 100	.4	1	30, 50
.8	2	16, 40, 60, 100			

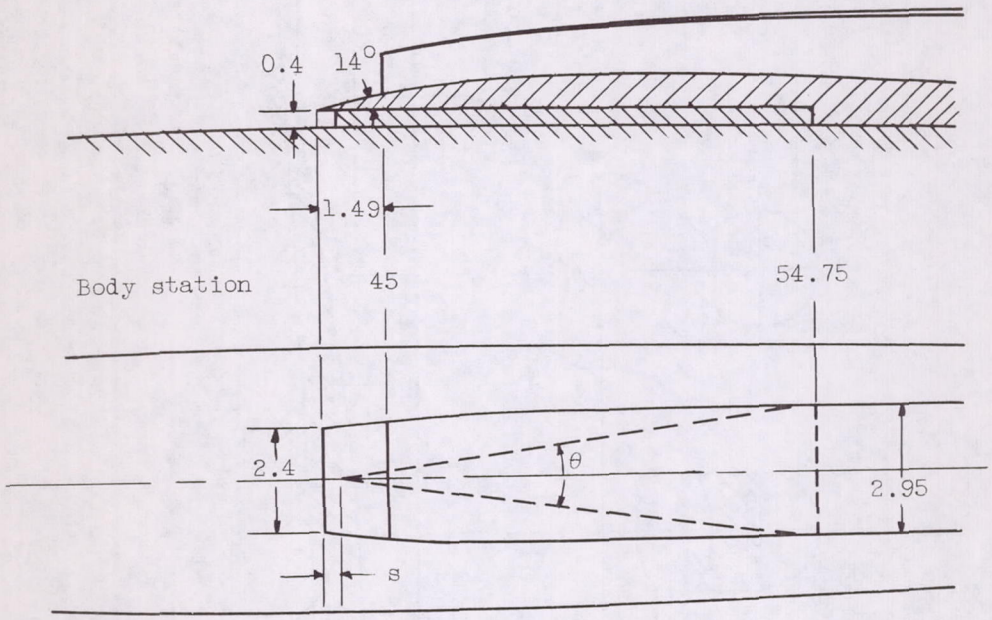

(a) Closed wedge.

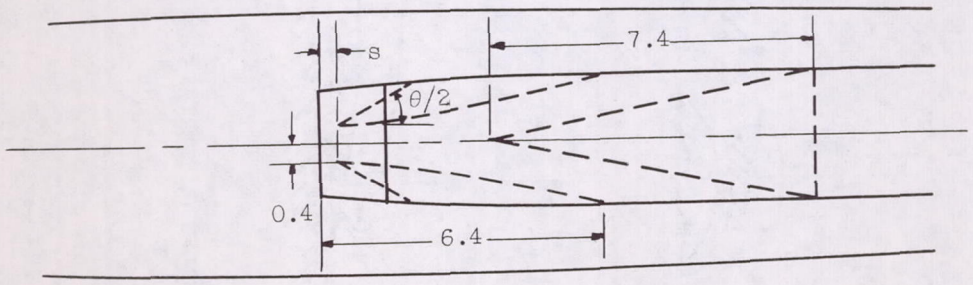

(b) Ducted wedge.

Figure 2. - Boundary-layer-removal wedge configurations. (Dimensions are in inches.)

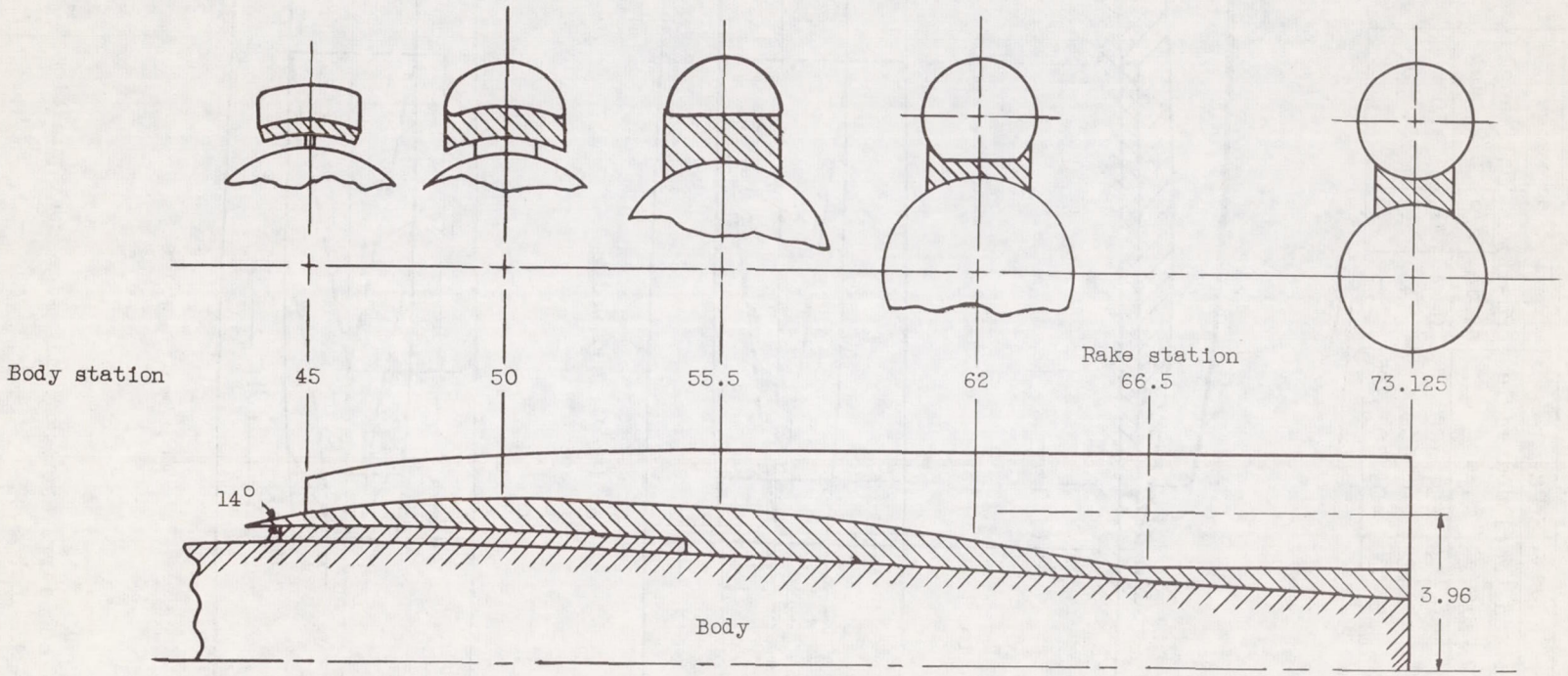

Figure 3. - Details of inlet. (Dimensions are in inches.)

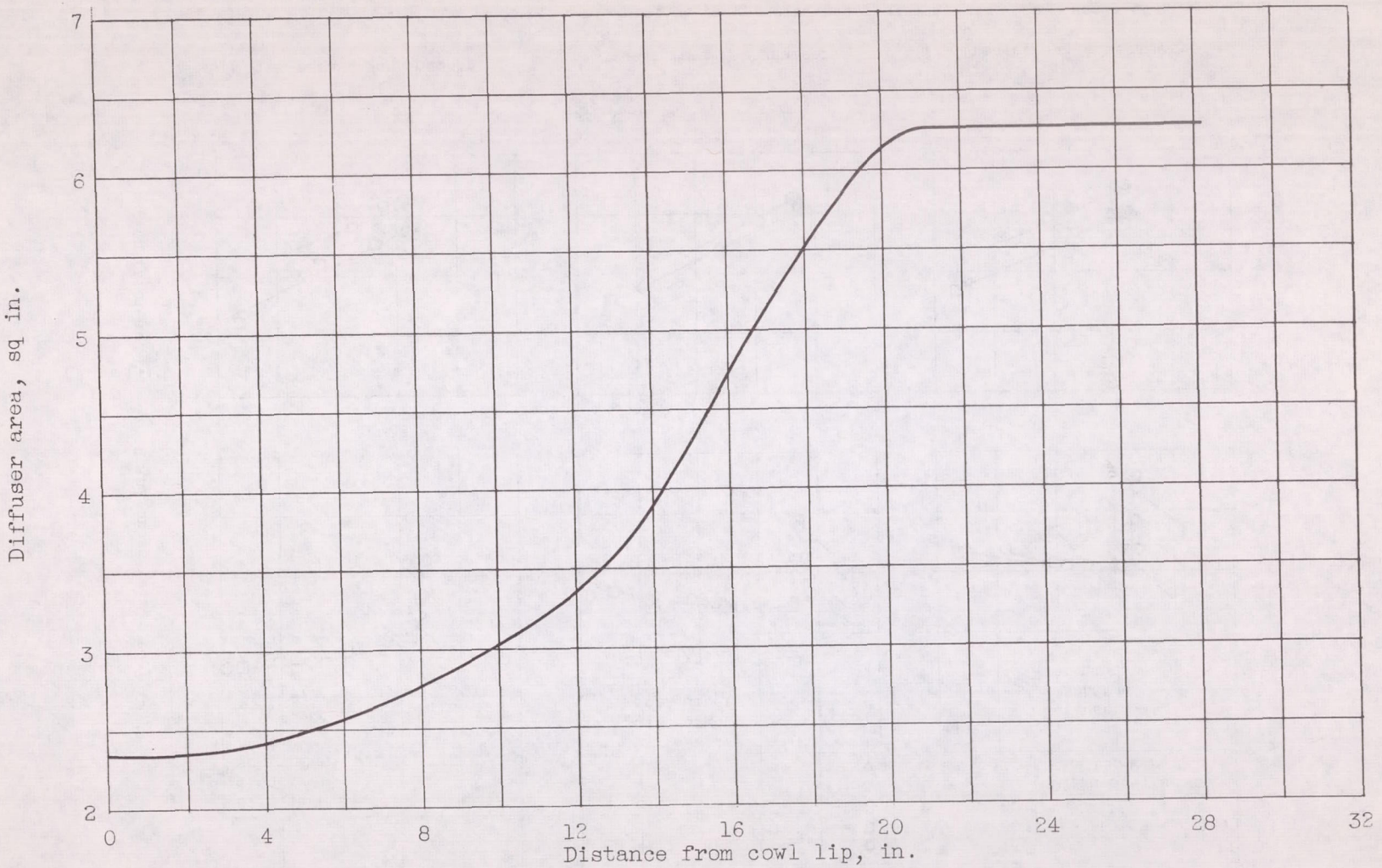

Figure 4. - Variation of subsonic-diffuser area.

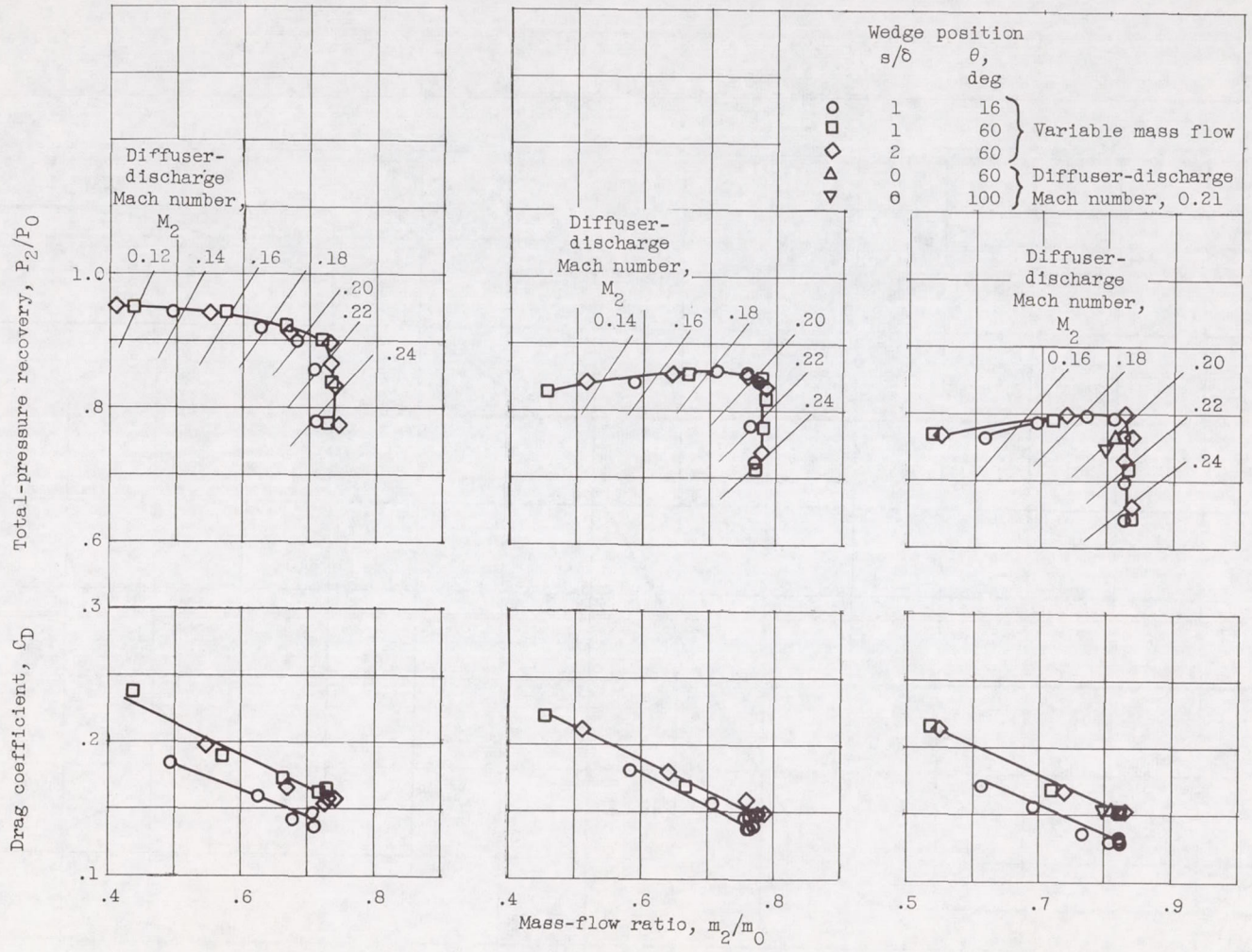

(a) Free-stream Mach number, 1.5.

(b) Free-stream Mach number, 1.8.

(c) Free-stream Mach number, 2.0.

Figure 5. - Effect of closed-wedge configuration on pressure recovery and drag. Zero angle of attack.

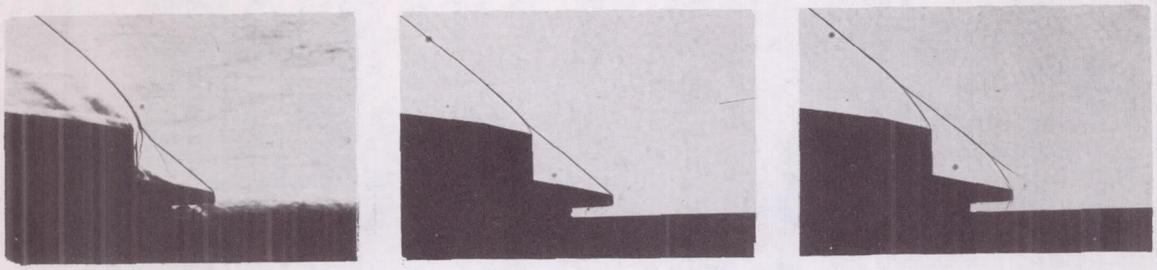

Included angle, 16° Included angle, 40° Included angle, 100°

(a) Closed wedges. Longitudinal wedge position s/δ of 2.

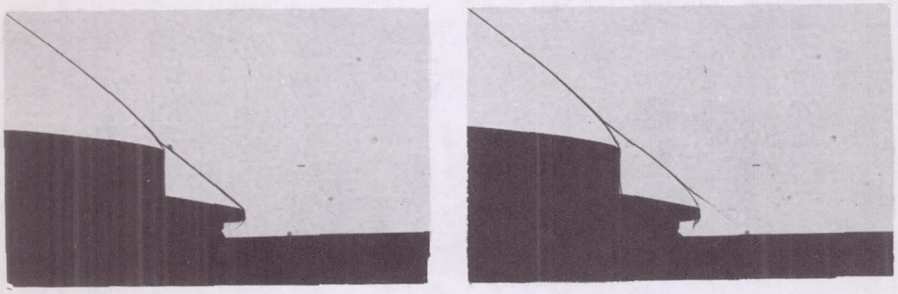

Included angle, 16° Included angle, 60°

(b) Closed wedges. Longitudinal wedge position s/δ of 1.

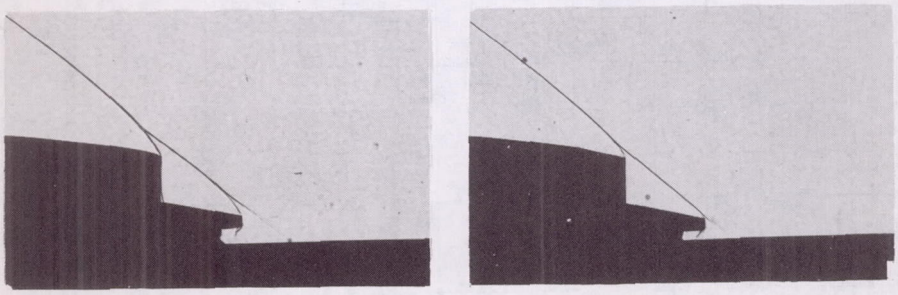

C-35289

Closed; included angle, 60° Ducted; half angle, 30°

(c) Closed and ducted wedges. Longitudinal wedge position s/δ of 1.

Figure 6. - Schlieren photographs of several diverter configurations. Free-stream Mach number, 2.0; zero angle of attack.

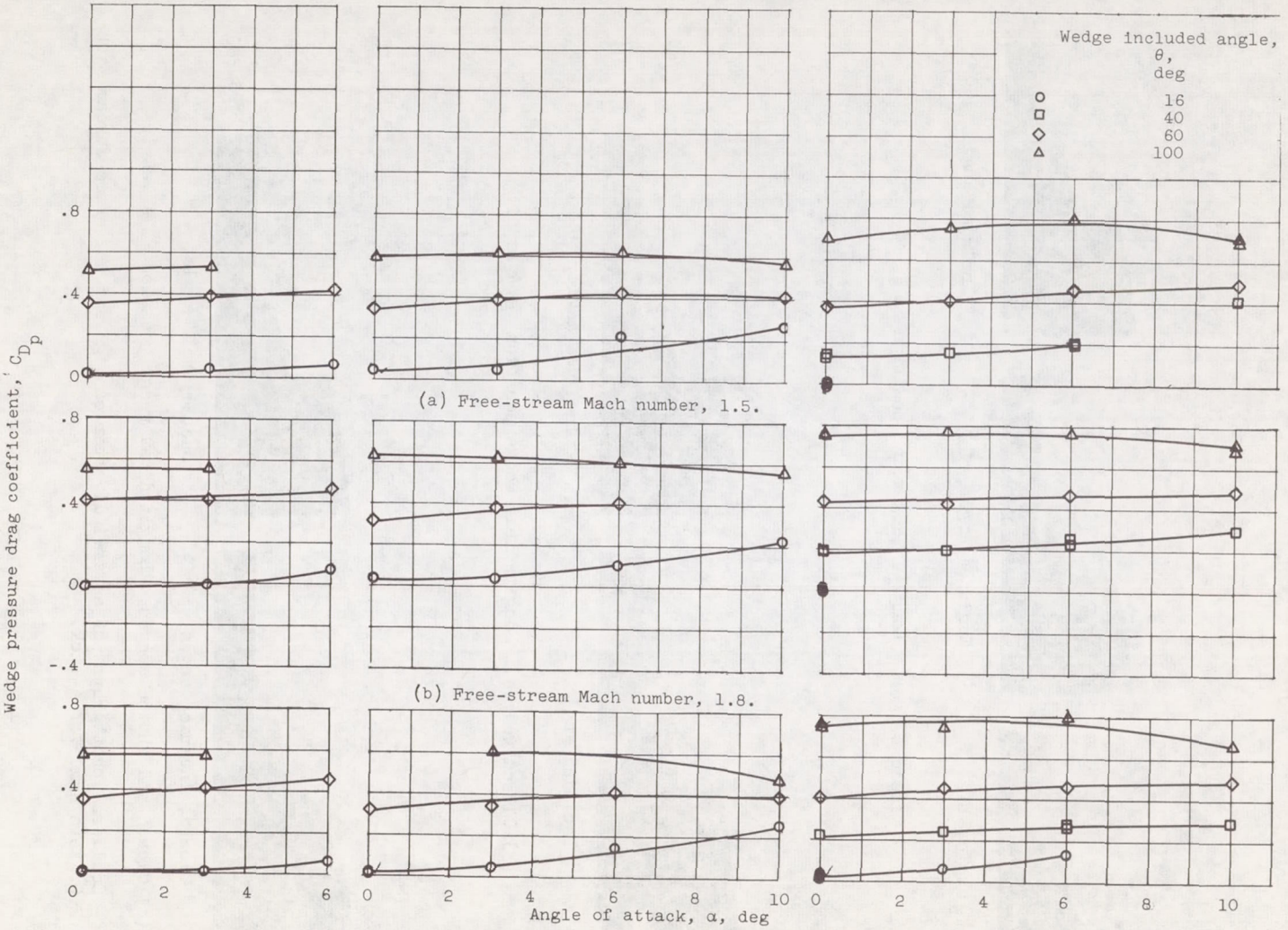

(a) Free-stream Mach number, 1.5.

(b) Free-stream Mach number, 1.8.

(c) Free-stream Mach number, 2.0.

Figure 7. - Wedge pressure drag coefficients for closed wedges.

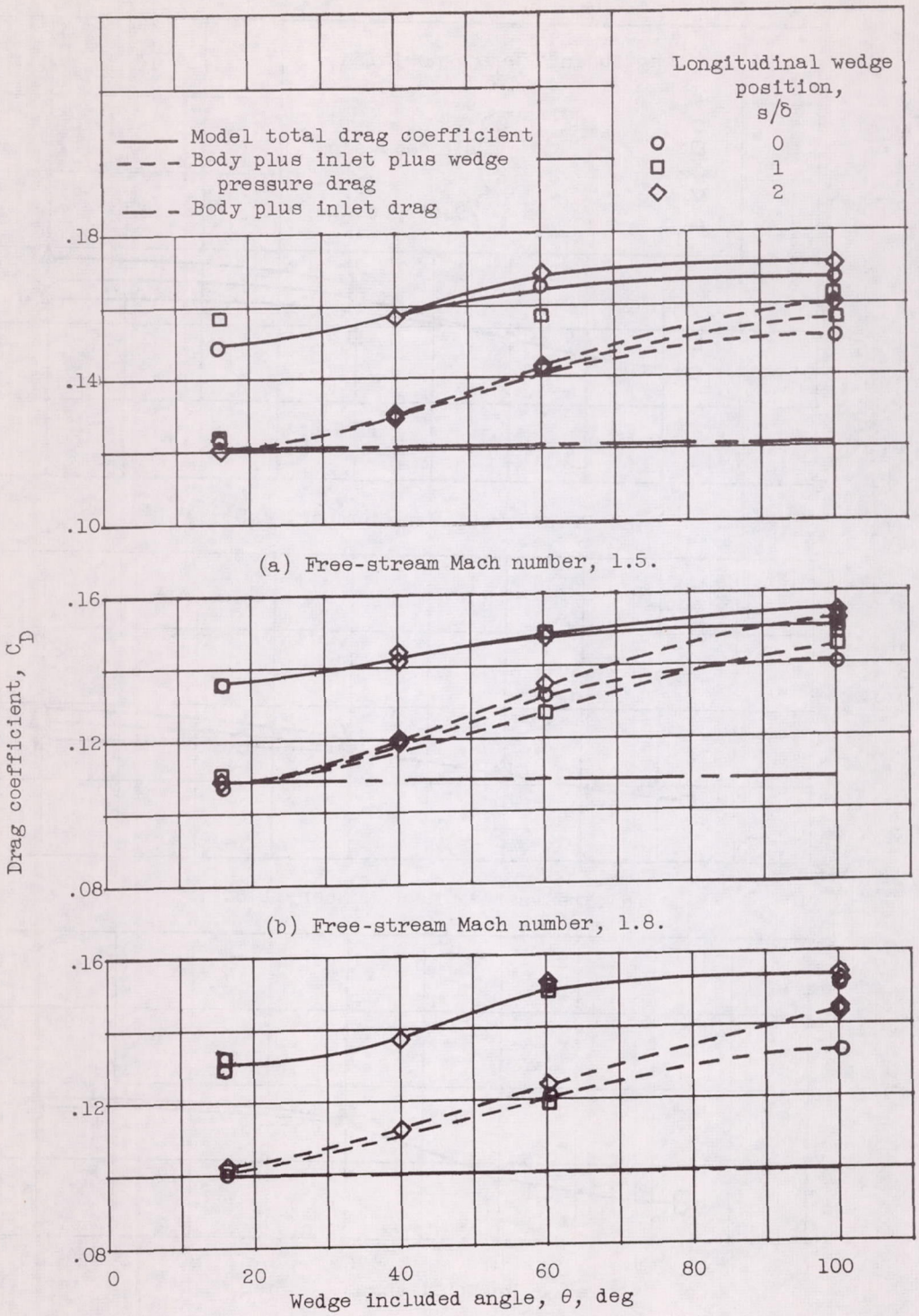

Figure 8. - Effect of wedge angle on diverter component drags. Diffuser-discharge Mach number, 0.21; zero angle of attack.

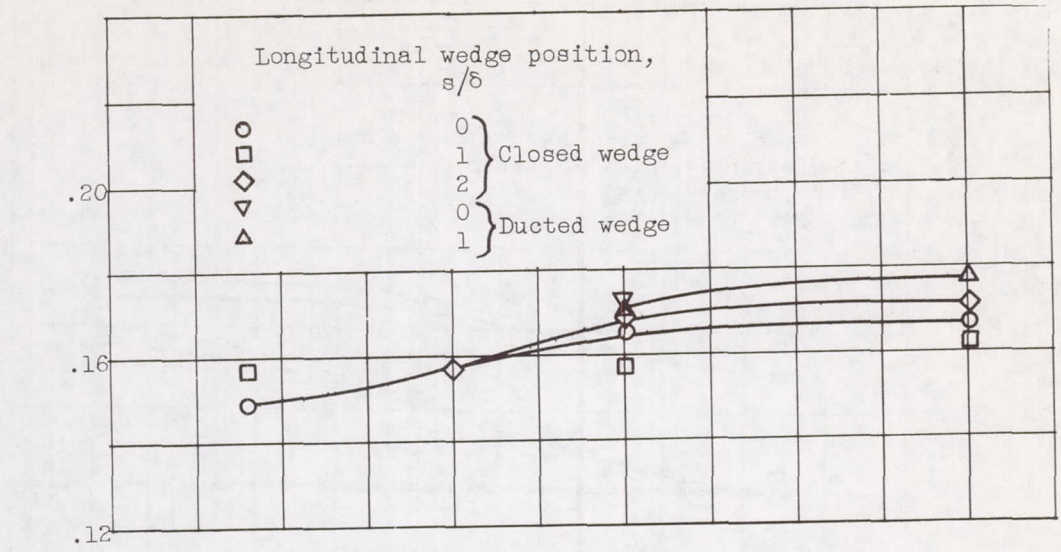

(a) Free-stream Mach number, 1.5.

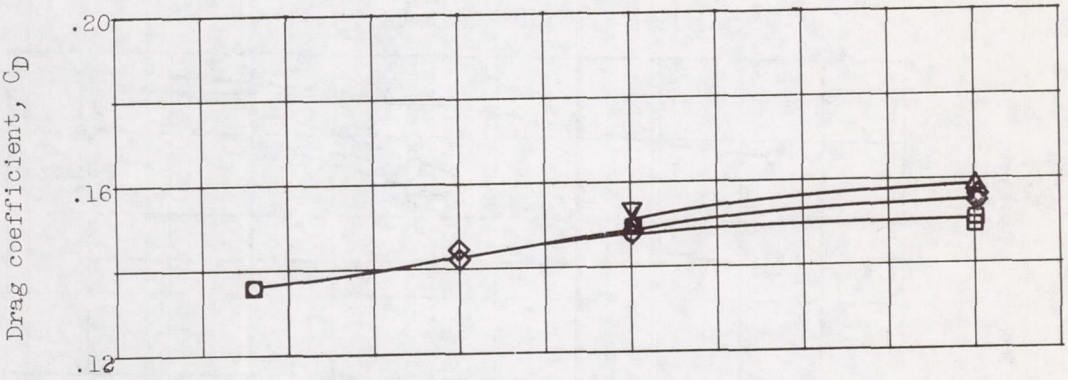

(b) Free-stream Mach number, 1.8.

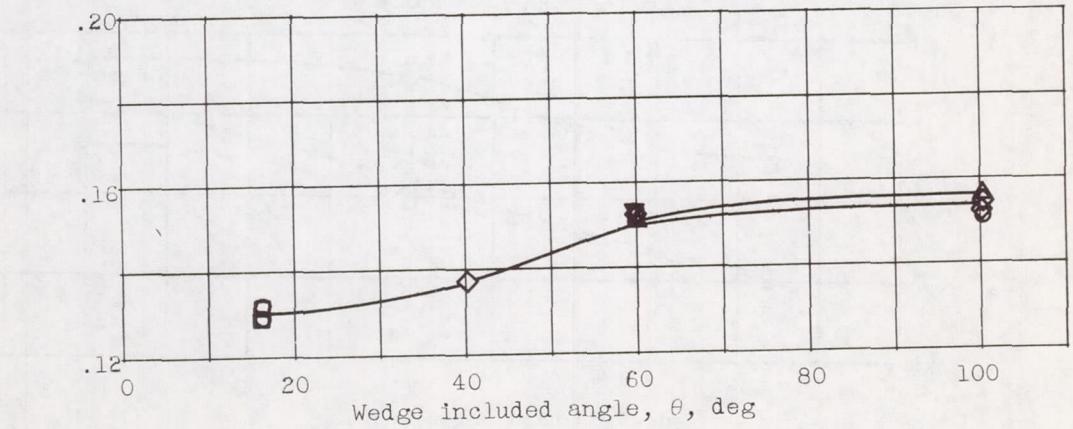

(c) Free-stream Mach number, 2.0.

Figure 9. - Comparison of drag coefficients for closed- and ducted-wedge diverters. Diffuser-discharge Mach number, 0.21; zero angle of attack.